Journal of Solid State Chemistry **150,** 316–323 (2000)
doi:10.1006/jssc.1999.8596, available online at http://www.idealibrary.com on IDEAL®

Structure Determination of $Sr_{1.25}Bi_{0.75}O_3$ and $Sr_{0.4}K_{0.6}BiO_3$ as a Function of Temperature from Synchrotron X-Ray Powder Diffraction Data

C. Bougerol-Chaillout,*,[1] P. Bordet,* S. M. Kazakov,† J. S. Pshirkov,† E. V. Antipov,† S. N. Putilin,† E. Dooryhee,‡ and A. Fitch‡

*Laboratoire de Cristallographie, CNRS-UJF, BP 166, 38042 Grenoble cedex 9, France; †Chemistry Department, Moscow State University, 119899 Moscow, Russia; and ‡ESRF, BP 220, 38043 Grenoble cedex, France

Received September 20, 1999; in revised form November 23, 1999; accepted December 4, 1999

The structures of $Sr_{1.25}Bi_{0.75}O_3$ and superconducting $Sr_{0.4}K_{0.6}BiO_3$ have been determined from synchrotron X-ray powder diffraction data between 4 K and the decomposition temperature, at 973 and 573 K, respectively. The symmetry remains monoclinic ($a \approx \sqrt{2}a_p$, $b \approx \sqrt{2}a_p$, $c \approx 2a_p$, $\beta \approx 90°$, $P2_1/n$ space group with two Bi sites allowing charge localization) for the undoped compound, and tetragonal ($a \approx \sqrt{2}a_p$, $c \approx 2a_p$, $I4/mcm$ space group with a unique Bi site implying a charge delocalization) for the K-doped phase, over the whole temperature range. In both cases the distortion from cubic symmetry decreases as temperature increases. Above 400 K, $Sr_{0.4}K_{0.6}BiO_3$ progressively loses oxygen until it reaches the $Sr_{0.4}K_{0.6}BiO_{2.5}$ stoichiometry, after which it decomposes. © 2000 Academic Press

Key Words: **mixed bismuth-based oxide; superconductivity; synchrotron powder X-ray diffraction; high temperature structure; low temperature structure.**

INTRODUCTION

Ten years after the report of superconductivity at ≈ 20 K in $Ba_{1-x}K_xBiO_3$ by Mattheiss *et al.* (1), we have discovered a second family of superconducting bismuthates, $Sr_{1-x}K_xBiO_3$ (2). Due to the much smaller ionic radius of Sr compared to that of Ba, the stabilization of the perovskite type phase $ABiO_3$ (A = Sr, K) was not straightforward and required the use of pressure. First, a sample of nominal composition $SrBiO_3$ was obtained under oxygen pressure (100 bar at 800°C); then, by synthesis under high pressure and at high temperature in a belt-type apparatus, $Sr_{1-x}K_xBiO_3$ samples were prepared, showing superconductivity in the $x = 0.45$–0.6 composition range with $T_{c,max} \approx 12$ K.

The structure of $Sr_{1-x}K_xBiO_3$ with $x = 0$ and 0.6 was determined at room temperature from powder neutron diffraction data. As for the Ba-based analogs, $Ba_{1-x}K_xBiO_3$ (3) and $BaPb_{1-x}Bi_xO_3$ (4), the structure is based on a perovskite-type arrangement. The structure of $SrBiO_3$ was described in the monoclinic $P2_1/n$ space group ($a \approx \sqrt{2}a_p$, $b \approx \sqrt{2}a_p$, $c \approx 2a_p$, $\beta \approx 90°$, $Z = 4$), which allows two distinct crystallographic sites for the Bi cations and therefore a charge disproportionation between Bi^{3+} and Bi^{5+}, in agreement with the semiconducting properties of the compound. In contrast, the superconducting phase $Sr_{0.4}K_{0.6}BiO_3$ crystallizes in the tetragonal $I4/mcm$ space group ($a \approx \sqrt{2}a_p$, $c \approx 2a_p$, $Z = 4$), where only one Bi site exists.

For the Ba-based phases, the structure is known to change as a function of temperature (3). In order to establish the structural phase diagram in the case of the Sr-based phases and to check for a possible structural phase transition below T_c for superconducting samples, powder X-ray diffraction data were collected at the BM16 ESRF beam line on $SrBiO_3$ and $Sr_{0.4}K_{0.6}BiO_3$ samples from room temperature down to 4 K and up to 973 K. The results from the structural analysis are reported herein.

EXPERIMENTAL

1. Synthesis and Samples Characterization

$SrBiO_3$ was prepared from $Sr_2Bi_2O_5$ heated for 35 h at 800°C under 100 bar of oxygen pressure. We noticed that when $SrBiO_3$ was used as the nominal composition, impurities were always present, such as $SrBi_3O_x$ (5), indicating that the starting composition was too rich in Bi. We then studied the solid solution $Sr_{1+x}Bi_{1-x}O_3$ with $0 < x < 0.3$ and found that monophasic samples were obtained only for $x \approx 0.2$ (6).

[1] To whom correspondence should be addressed. E-mail: bougerol@polycnrs-gre.fr.

0022-4596/00 $35.00

$Sr_{0.4}K_{0.6}BiO_3$ was prepared by a high-pressure, high-temperature technique in a belt-type apparatus, using Au capsules, at 2GPa and 700°C for 1 h as reported in (2).

Since the samples used for the low temperature experiment presented impurities, other batches were prepared for the following high temperature experiment with an excess of 5% of KO_2 in order to compensate its probable lack due to a reaction with the container in strongly oxidizing conditions. The samples turned out to be single phases.

The cationic composition of the samples was checked by EDS analysis in a transmission electron microscope (Philips CM300) equipped with a Kevex analysis system.

The superconducting transition temperature T_c (12 K) and the superconducting volume fraction (about 40%) were determined from a.c. susceptibility and resistivity measurements.

2. Data Collection

Data were collected at the BM16 beam line of the ESRF using a Si(111) double-crystal monochromator and a multi-analyzer stage comprising nine Ge(111) analyzer crystals with a 2° angular separation and nine scintillation counters. The wavelength was calibrated using a silicon standard, yielding 0.41334 and 0.35112 Å for the low and high temperature experiments, respectively.

Samples were mounted in quartz capillaries (diameter 0.5 mm). For the low temperature experiment down to 4 K, a helium flow cryostat allowing sample rotation was used. Helium gas was introduced inside the sample chamber to ensure a good temperature exchange. For the high temperature experiment, a high temperature gas blower was used, and the sample was attached to a spinner mounted on the diffractometer. The temperature stability was better than 0.1 K in all cases.

Data were recorded in a continous scan mode up to 30° (2θ). Countings from the nine detectors were then rebinned in 2θ steps of 0.005°, shifted to correct for the angular separation of the analyzer crystals, and summed. The minimum reflexion widths observed in the resulting spectra were $\approx 0.02°$ (2θ).

3. Refinement Procedure

The structural refinements were carried out with the Rietveld method, using the FULPROF program (7). The peak shape was modeled with a pseudo Voigt function convoluted with the axial divergence asymmetry correction proposed by Finger *et al.* (8). The background was described as a polynomial function of the fifth order. The data were corrected for cylindrical absorption using the experimentally determined packing density of the powder. During the low temperature measurements of the $Sr_{0.4}K_{0.6}BiO_3$ sample, the basis of the capillary broke and a small part of the powder was progressively sucked out from the capillary by the cryostat vacuum. This resulted in an inaccuracy of the absorption correction, which may explain the unphysical values of the thermal parameters obtained from the refinements of the low temperature data. However, cell and positional parameters should not be markedly affected by this effect. The structural models used as the starting points of the refinements were those reported in (2). The bond distances were calculated with the BONDSTR program (7).

RESULTS AND DISCUSSION

1. $Sr_{1+x}Bi_{1-x}O_3$

a. Low temperature. The sample used for this experiment, of nominal composition $SrBiO_3$, presented two impurity phases, $SrBi_3O_x$ (12%) and $SrBi_2O_4$ (3%), which were introduced into the refinement.

In order to refine the structure as accurately as possible, data were first collected at room temperature without the cryostat, then they were collected at 150, 100, and 20 K. When neutron data was used for the structure refinement (2), two space groups, orthorhombic *Pbnm* or monoclinic $P2_1/n$ were considered. The choice of $P2_1/n$, allowing 2 Bi sites contrary to *Pbnm*, had been motivated more by the physical properties than by a real improvement of the fit. In the case of room temperature synchrotron data, the symmetry appeared clearly monoclinic with a refined β angle of 90.0417 (9)° and furthermore, the (011) reflexion allowed in $P2_1/n$ but not in *Pbnm* was undoubtedly visible. The Bi cations occupy two distinct octahedral sites, named Bi1 and Bi2 (Fig. 1a). During the refinement, we found that the temperature factor of Bi1 was anomalously large compared to that of Bi2. We thought that this might be due to the presence of Sr on that site. Therefore, we constrained both temperature factors to be equal, introduced Sr on Bi1 site, and refined the Sr/Bi ratio. We found that the Bi1 site was occupied by 75% of Bi and 25% of Sr, whereas the Sr and Bi2 sites were fully occupied by Sr and Bi, respectively. The deduced composition of the sample was $Sr_{1.25(1)}Bi_{0.75(1)}O_3$. Later on, EDS analysis in a transmission electron microscope confirmed this stoichiometry, and, as mentioned in the experimental part above, single phase samples could then be obtained by starting from this nominal composition. It should be mentioned that the deviation from 1 : 1 for the Sr/Bi ratio had not been observed previously in the neutron diffraction experiment due to the similarity in the scattering factors of Sr and Bi for neutrons. The structural parameters, after convergence had been reached, are reported in Table 1 and the main interatomic distances are reported in Table 2. They are in good agreement with the parameters reported previously in (2). The average Bi1–O and Bi2–O distances are 2.29(4) and 2.13(4) Å, respectively, which reveals a large difference in the size of the two sites. From these values and the constants reported in (9), the Bi valence has been

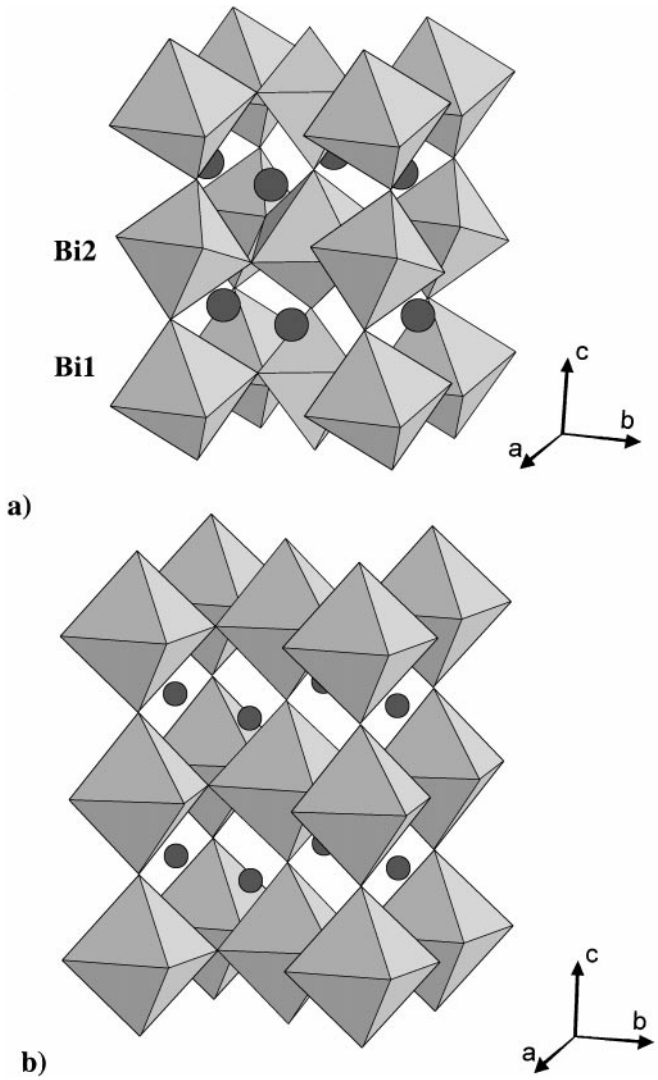

FIG. 1. Structure of (a) $Sr_{1.25}Bi_{0.75}O_3$ and of (b) $Sr_{0.4}K_{0.6}BiO_3$.

calculated using the bond length–bond strength method. For Bi2, a value of +5.0 was obtained. For Bi1, such a calculation could not be done since the site is partially occupied by Sr. However, these results indicate clearly a charge disproportionation and localization accounting for the semiconducting behavior of the compound.

The symmetry remains monoclinic with the same $P2_1/n$ space group down to 20 K. As can be seen in Fig. 2 (part A) a and c increase almost linearly as the temperature is raised with a comparable expansion coefficient ($\Delta a/a = 3.4\ 10^{-3}$/K and $\Delta c/c = 3.2\ 10^{-3}$/K), whereas b remains almost constant over the whole temperature range. The average Bi1–O and Bi2–O distances remain constant as well, within the standard deviations.

b. High temperature. For this experiment, we used a new sample of nominal stoichiometry $Sr_{1.25}Bi_{0.75}O_3$ which appeared single phase. Data were collected at 303, 373, and every 50 K until 973 K at which temperature the sample decomposed. At each temperature, and besides the scale factor and the profile parameters, we refined the lattice parameters, the variable atomic coordinates, and the isotropic temperature factors. The Sr content on Bi1 site was refined at 303 K. The value obtained (28%) was kept constant at higher temperatures. The results after convergence are reported in Table 3. The symmetry remains monoclinic with the $P2_1/n$ space group over the whole temperature range. Figure 3 shows the diffractogram corresponding to the 303 K experimental data as well as the calculated spectrum and the difference between them. The a, b, and c lattice parameters increase linearly with temperature (Fig. 2, part B). The monoclinic angle β increases slightly up to 773 K, after which it saturates around 90.07°. The ratios c/a, c/b, and a/b vary with increasing temperature in such a way that the distortion from cubic-related parameters ($a = b = \sqrt{2}a_p$, $c = 2a_p$) decreases (Fig. 4). For each Bi octahedral site, the six Bi–O distances are very close. The

TABLE 1
Positional and Thermal Parameters for $Sr_{1.25}Bi_{0.75}O_3$ at Room Temperature, 150, 100, and 20 K (Space Group $P2_1/n$)

T (K)		Room T	150	100	20
a (Å)		5.94761(2)	5.93380(4)	5.93038(4)	5.92795(3)
b (Å)		6.09707(2)	6.09507(4)	6.09562(4)	6.09611(3)
c (Å)		8.48555(3)	8.46768(5)	8.46317(6)	8.45958(5)
β (°)		90.0417(9)	90.033(2)	90.045(1)	90.046(1)
Sr 4*e*	*x*	−0.0138(7)	−0.0145(9)	−0.0121(9)	−0.0141(8)
	y	0.5466(2)	0.5479(3)	0.5482(3)	0.5495(2)
	z	0.2496(7)	0.2497(8)	0.2486(8)	0.2494(8)
	B (Å²)	0.45(4)	0.15(5)	0.44(5)	0.20(4)
Bi1 (Sr) 2*a*	*x*	0	0	0	0
	y	0	0	0	0
	z	0	0	0	0
	B (Å²)	0.29(7)	0.30(8)	0.94(8)	0.29(7)
Bi2 2*b*	*x*	0	0	0	0
	y	0	0	0	0
	z	0.5	0.5	0.5	0.5
	B (Å²)	0.10(5)	−0.02(6)	0.15(6)	0.09(6)
O1 4*e*	*x*	0.402(2)	0.400(3)	0.396(3)	0.403(2)
	y	0.461(2)	0.458(3)	0.456(3)	0.460(2)
	z	0.247(4)	0.261(5)	0.261(5)	0.247(4)
	B (Å²)	1.1(2)	1.2(4)	0.8(4)	0.8(3)
O2 4*e*	*x*	0.280(4)	0.265(5)	0.261(5)	0.267(5)
	y	0.195(3)	0.186(4)	0.183(4)	0.192(4)
	z	0.536(4)	0.539(6)	0.546(6)	0.549(5)
	B (Å²)	1.1(2)	1.2(4)	0.8(4)	0.8(3)
O3 4*e*	*x*	0.191(4)	0.193(5)	0.186(5)	0.189(4)
	y	0.720(4)	0.727(5)	0.735(5)	0.723(4)
	z	0.565(3)	0.553(5)	0.549(5)	0.548(4)
	B (Å²)	1.1(2)	1.2(4)	0.8(4)	0.8(3)
R_{wp} (%)		8.7	10.7	11.9	9.4
R_{Bragg} (%)		3.8	4.5	6.5	3.5
χ^2		2.1	4.8	9.1	12.1

Note. The Sr content on the Bi1 site was refined at room temperature and the value was kept constant at others temperatures.

TABLE 2
Bi–O Interatomic Distances (Å) for $Sr_{1.25}Bi_{0.75}O_3$ from 20 to 923 K

T (K)	923	873	823	773	723	673	623	573	523	473	423	373	303	293	150	100	20
Bi1–O1 × 2	2.34(4)	2.36(3)	2.35(3)	2.37(3)	2.31(3)	2.37(3)	2.35(3)	2.34(3)	2.27(4)	2.34(3)	2.28(4)	2.33(4)	2.41(3)	2.23(3)	2.12(3)	2.13(4)	2.23(3)
Bi1–O2 × 2	2.36(4)	2.33(3)	2.31(3)	2.33(3)	2.32(3)	2.33(3)	2.32(4)	2.35(3)	2.35(3)	2.37(3)	2.39(3)	2.41(3)	2.45(3)	2.29(2)	2.39(3)	2.43(3)	2.37(3)
Bi1–O3 × 2	2.38(4)	2.43(4)	2.48(3)	2.41(3)	2.40(3)	2.41(3)	2.42(3)	2.41(3)	2.37(3)	2.39(3)	2.42(4)	2.41(3)	2.40(3)	2.34(2)	2.33(3)	2.39(3)	2.33(2)
Average Bi1–O	2.36(7)	2.37(6)	2.38(5)	2.37(5)	2.34(5)	2.37(5)	2.36(6)	2.37(5)	2.33(6)	2.37(5)	2.36(6)	2.38(6)	2.42(5)	2.29(5)	2.28(5)	2.32(5)	2.31(5)
Bi2–O1 × 2	2.05(4)	2.04(3)	2.04(3)	2.03(3)	2.08(3)	2.04(3)	2.06(3)	2.06(3)	2.12(4)	2.06(3)	2.13(4)	2.07(4)	2.01(3)	2.19(3)	2.31(4)	2.31(4)	2.18(3)
Bi2–O2 × 2	2.08(4)	2.09(3)	2.11(3)	2.06(3)	2.08(3)	2.07(3)	2.08(4)	2.07(3)	2.04(4)	2.04(3)	2.03(3)	2.01(4)	1.96(3)	2.07(2)	1.97(3)	1.95(3)	2.01(3)
Bi2–O3 × 2	2.03(4)	2.05(4)	1.98(3)	2.06(3)	2.07(3)	2.06(3)	2.03(3)	2.02(3)	2.10(3)	2.06(3)	2.00(3)	2.01(3)	2.05(3)	2.12(2)	2.07(3)	2.00(3)	2.07(3)
Average Bi2–O	2.05(7)	2.06(6)	2.04(5)	2.05(5)	2.08(5)	2.06(5)	2.06(6)	2.05(5)	2.09(6)	2.05(5)	2.05(6)	2.03(6)	2.01(5)	2.13(5)	2.12(5)	2.09(5)	2.09(5)

average Bi1–O and Bi2–O distances remained constant within the standard deviations at 2.37 and 2.05 Å, respectively, from room temperature to decomposition temperature (Table 2).

2. $Sr_{0.4}K_{0.6}BiO_3$

a. Low temperature. Data were collected at room temperature, 150, 20, and 4 K. The sample used for this experiment contained a few percent of $KBiO_3$ as impurity, which was introduced as a second phase into the refinement (10). We also noticed that most reflexions presented anomalous shapes, which we attributed to a variation of the potassium composition in the sample. The Sr/K ratio refined at room temperature was found to be 2/3. At all temperatures the structure has been described in the tetragonal $I4/mcm$ space group reported in (2). The lattice parameters and the variable atomic coordinates after the last refinement cycle at each temperature are reported in Table 4. The results at room temperature confirm those reported from neutron data (2). The Bi cations occupy only one octahedral site (Fig. 1b), almost regular with two Bi–O1 = 2.1091(2) Å and four Bi–O2 = 2.112(2) Å. Since the average Bi valence calculated from the stoichiometry is + 4.6, the charges are necessarily delocalized, which accounts for the metallic behavior of the sample. The octahedra are tilted around the c axis by 6° from the ideal cubic-like position. This value is comparable to the tilt angle in the superconducting $BaPb_{0.75}Bi_{0.25}O_3$ (7°), which also crystallizes in the $I4/mcm$ space group. No structural change was observed below T_c (12 K). The a and c lattice parameters decrease with temperature (Fig. 5, part A), with an expansion coefficient along a ($\Delta a/a = 2.8 \times 10^{-3}$/K) larger than along c ($\Delta c/c = 1.0 \times 10^{-3}$/K). The Bi–O distances remain constant within the standard deviations with decreasing temperature (Table 5).

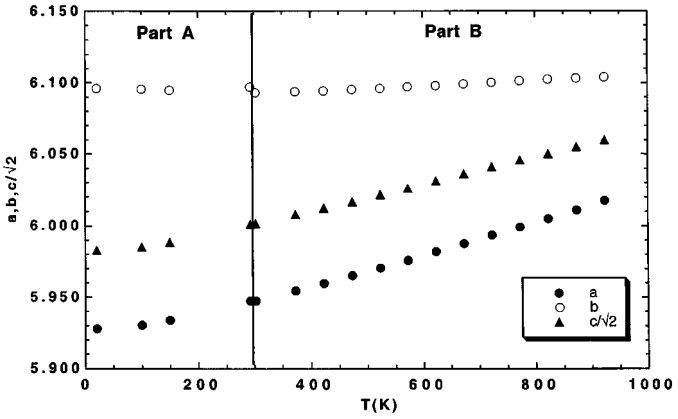

FIG. 2. Variation of a, b, and $c/\sqrt{2}$ as a function of temperature for $Sr_{1.25}Bi_{0.75}O_3$. Parts A and B correspond to the low and high temperature experiments, respectivley.

b. High temperature. Another sample was synthesized for this experiment, which appeared single phase until decomposition. Data were collected at 303, 373, and every 50 K up to 573 K, after which decomposition began. The symmetry remains tetragonal over the whole temperature range and the refinements have been carried out in the $I4/mcm$ space group. The Sr/K ratio was refined at 303 K and then kept constant for higher temperatures. The value obtained, 2/3, is in good agreement with the results from EDS analyses performed on the same sample in a transmission electron microscope.

As can be seen in Fig. 5 (part B), both a and c lattice parameters increase linearly as a function of temperature, and the c/a ratio decreases, coming closer to the $\sqrt{2}$ value which would correspond to a cubic symmetry. The final results of the refinements at all temperatures are reported in Table 6.

For the refinements carried out at 303 and 373 K, the temperature factors of the two apical O1 oxygen atoms (B(O1)) and of the four planar O2 atoms (B(O2)) were varied independently, but converged to similar values. When this procedure was used at higher temperatures, we noticed that B(O1) became much larger than B(O2) and increased quickly with temperature. Therefore, in a second step and from 423 to 573 K, we constrained B(O1) and B(O2) to be equal and refined the occupancy of the O1 site. Figure 6 shows

TABLE 3
Positional and Thermal Parameters for $Sr_{1.25}Bi_{0.75}O_3$ at High Temperatures (Space Group $P2_1/n$)

T (K)		303	373	423	473	523	573	623	673	723	773	823	873	923
a (Å)		5.94738(5)	5.95450(5)	5.95956(4)	5.96501(4)	5.97047(4)	5.97592(4)	5.98197(4)	5.98774(3)	5.99358(3)	5.99929(3)	6.00491(3)	6.01097(3)	6.01760(3)
b (Å)		6.09328(5)	6.09390(5)	6.09449(4)	6.09545(4)	6.09629(4)	6.09730(4)	6.09818(4)	6.09947(3)	6.10044(3)	6.10160(3)	6.10249(3)	6.10335(3)	6.10407(3)
c (Å)		8.48617(7)	8.49504(7)	8.50131(7)	8.50780(6)	8.51453(6)	8.52105(6)	8.52833(6)	8.53519(5)	8.54212(5)	8.54871(5)	8.55500(4)	8.56183(4)	8.56893(5)
β (°)		90.038(2)	90.041(2)	90.044(1)	90.056(1)	90.056(1)	90.0582(8)	90.0654(6)	90.0672(5)	90.0683(5)	90.0699(4)	90.0692(4)	90.0692(4)	90.0691(4)
Sr 4*e*	*x*	− 0.0136(9)	− 0.012(1)	− 0.012(1)	− 0.011(1)	− 0.010(1)	− 0.008(1)	− 0.009(1)	− 0.010(1)	− 0.009(1)	− 0.009(1)	− 0.009(1)	− 0.007(1)	− 0.006(2)
	y	0.5467(3)	0.5453(4)	0.5444(4)	0.5436(4)	0.5435(4)	0.5426(4)	0.5414(4)	0.5409(4)	0.5404(4)	0.5389(4)	0.5381(5)	0.5371(5)	0.5360(5)
	z	0.249(1)	0.251(1)	0.2488(9)	0.2493(9)	0.2475(8)	0.2497(8)	0.2491(8)	0.2492(7)	0.2488(8)	0.2497(8)	0.2491(8)	0.2498(8)	0.2499(9)
	B (Å^2)	1.08(5)	1.01(6)	1.06(6)	1.22(6)	1.47(6)	1.63(5)	1.64(6)	1.84(5)	2.03(6)	2.12(6)	2.26(6)	2.46(6)	2.69(7)
Bi1 (Sr) 2*a*	*x*	0	0	0	0	0	0	0	0	0	0	0	0	0
	y	0	0	0	0	0	0	0	0	0	0	0	0	0
	z	0	0	0	0	0	0	0	0	0	0	0	0	0
	B (Å^2)	0.85(7)	0.63(8)	0.74(7)	0.80(7)	0.92(7)	0.99(6)	1.09(6)	1.20(6)	1.19(6)	1.35(6)	1.48(6)	1.59(6)	1.71(7)
Bi2 2*b*	*x*	0	0	0	0	0	0	0	0	0	0	0	0	0
	y	0	0	0	0	0	0	0	0	0	0	0	0	0
	z	0.5	0.5	0.5	0.5	0.5	0.5	0.5	0.5	0.5	0.5	0.5	0.5	0.5
	B (Å^2)	0.71(5)	0.40(6)	0.42(5)	0.44(5)	0.52(5)	0.59(5)	0.59(4)	0.68(4)	0.82(5)	0.85(4)	0.89(4)	0.97(4)	1.05(5)
O1 4*e*	*x*	0.407(3)	0.416(3)	0.416(3)	0.419(4)	0.420(4)	0.418(3)	0.419(4)	0.421(3)	0.424(4)	0.421(3)	0.426(4)	0.425(4)	0.422(4)
	y	0.455(3)	0.453(3)	0.451(3)	0.457(3)	0.458(3)	0.455(3)	0.451(3)	0.459(3)	0.464(3)	0.467(4)	0.463(4)	0.465(4)	0.473(5)
	z	0.226(3)	0.235(4)	0.236(4)	0.233(4)	0.240(5)	0.233(4)	0.232(4)	0.230(3)	0.236(4)	0.232(3)	0.231(4)	0.231(5)	0.233(4)
	B (Å^2)	0.7(3)	1.1(4)	1.4(4)	1.8(4)	2.1(4)	2.3(6)	1.7(5)	2.2(5)	2.9(6)	2.5(6)	2.9(5)	2.5(7)	3.2(8)
O2 4*e*	*x*	0.248(5)	0.257(6)	0.253(6)	0.260(6)	0.253(6)	0.263(6)	0.270(6)	0.263(5)	0.266(5)	0.252(5)	0.263(5)	0.254(5)	0.256(7)
	y	0.193(4)	0.195(5)	0.200(5)	0.202(5)	0.210(5)	0.205(5)	0.204(6)	0.206(5)	0.205(5)	0.220(5)	0.214(6)	0.219(5)	0.211(6)
	z	0.561(4)	0.562(5)	0.563(5)	0.559(5)	0.557(5)	0.561(5)	0.552(6)	0.553(5)	0.552(5)	0.561(4)	0.558(5)	0.562(4)	0.563(5)
	B (Å^2)	0.7(3)	1.1(4)	1.4(4)	1.8(4)	2.1(4)	2.3(6)	1.7(5)	2.2(5)	2.9(6)	2.5(6)	2.9(5)	2.5(7)	3.2(8)
O3 4*e*	*x*	0.179(4)	0.179(5)	0.180(5)	0.180(5)	0.182(5)	0.174(5)	0.180(5)	0.171(5)	0.174(5)	0.159(6)	0.155(6)	0.161(6)	0.166(7)
	y	0.724(5)	0.731(6)	0.732(5)	0.722(5)	0.717(5)	0.722(5)	0.730(5)	0.715(5)	0.716(5)	0.716(6)	0.717(5)	0.709(6)	0.710(7)
	z	0.557(4)	0.554(5)	0.555(5)	0.555(5)	0.559(6)	0.546(6)	0.560(5)	0.551(4)	0.552(5)	0.546(5)	0.536(5)	0.537(5)	0.500(6)
	B (Å^2)	0.7(3)	1.1(4)	1.4(4)	1.8(4)	2.1(4)	2.3(6)	1.7(5)	2.2(5)	2.9(6)	2.5(6)	2.9(5)	2.5(7)	3.2(8)
R_{wp} (%)		14.4	15.4	14.4	14.4	14.2	13.7	13.5	12.7	13.0	12.8	13.6	13.5	14.1
R_{Bragg} (%)		5.6	5.4	5.1	5.0	5.5	5.4	5.4	5.2	5.1	5.6	6.0	5.6	6.2

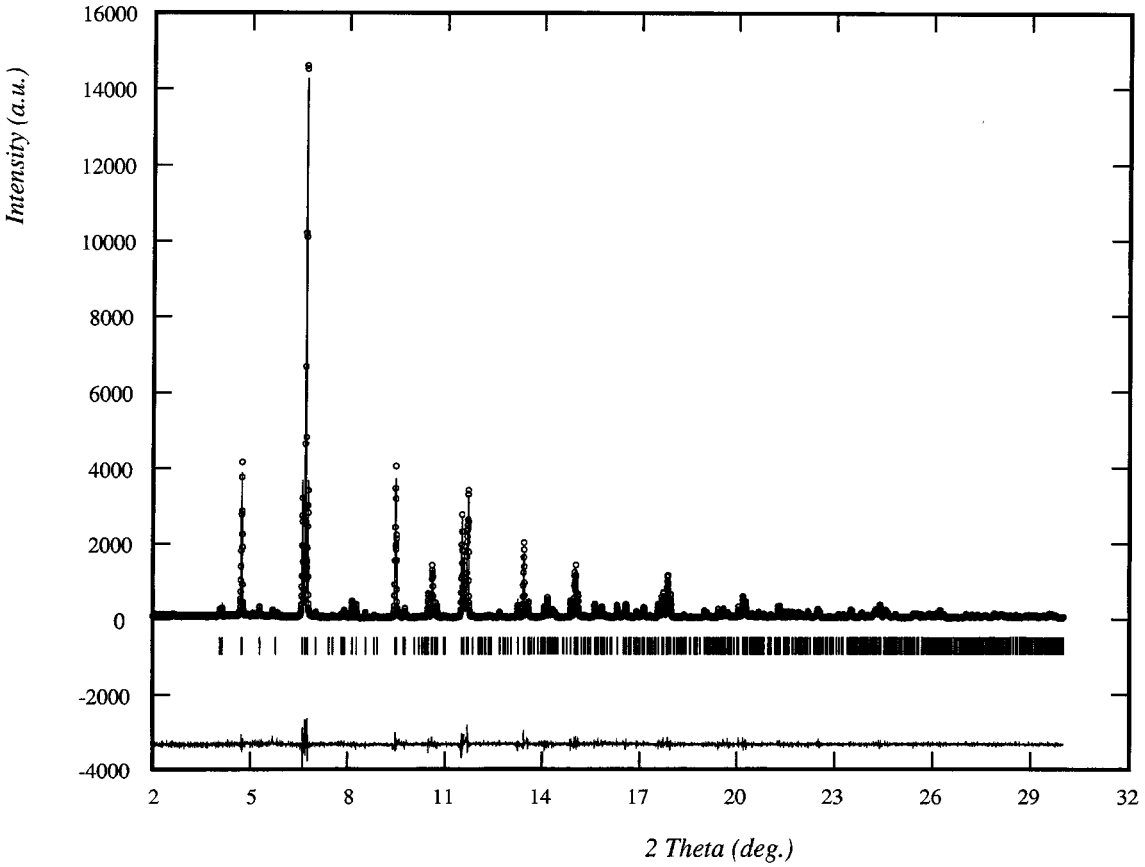

FIG. 3. Diffractogram taken at 303 K on $Sr_{1.25}Bi_{0.75}O_3$.

a regular decrease of this occupancy between 373 and 573 K, the temperature at which the O1 site is only half occupied. There is no obvious reason why the oxygen loss concerns O1 and not O2. However, in the closely related system $BaBiO_3$, we have also observed that the oxygen loss at high temperature concerned the O1-type position (11).

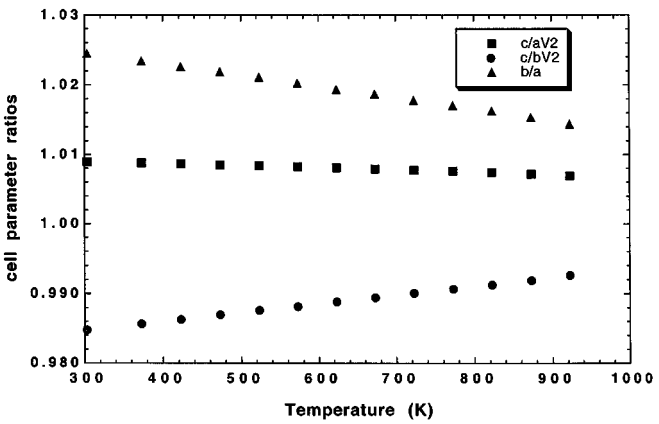

FIG. 4. Variation of the $c/a\sqrt{2}$, $c/b\sqrt{2}$, and a/b ratios for $Sr_{1.25}Bi_{0.75}O_3$ between room temperature and 923 K.

TABLE 4
Positional and Thermal Parameters for $Sr_{0.4}K_{0.6}BiO_3$ at Room Temperature, 150, 25, and 4 K (Space Group *I4/mcm*)

T (K)		Room *T*	150	25	4
a (Å)		5.93973(5)	5.92803(5)	5.92318(6)	5.92257(5)
c (Å)		8.43594(5)	8.4301(1)	8.4270(1)	8.42637(9)
Sr (K) 4*b*	*x*	0	0	0	0
	y	0.5	0.5	0.5	0.5
	z	0.25	0.25	0.25	0.25
	B (Å^2)	0.81(5)	0.98(7)	0.49(7)	− 0.17(4)
Bi 4*c*	*x*	0	0	0	0
	y	0	0	0	0
	z	0	0	0	0
	B (Å^2)	0.04(2)	− 0.37(2)	− 0.69(2)	− 0.71(2)
O1 4*a*	*x*	0	0	0	0
	y	0	0	0	0
	z	0.25	0.25	0.25	0.25
	B (Å^2)	2.8(9)	0.2(5)	− 0.3(5)	0.1(3)
O2 8*h*	*x*	0.224(3)	0.223(4)	0.221(3)	0.226(4)
	y	0.724(3)	0.723(4)	0.721(3)	0.726(4)
	z	0	0	0	0
	B (Å^2)	1.4(5)	2.3(5)	1.4(5)	0.1(3)
R_{wp} (%)		16.6	15.4	15.7	12.9
R_{Bragg} (%)		3.59	4.82	5.49	4.75

Note. The Sr/K ratio was refined at room temperature and kept constant at lower temperatures.

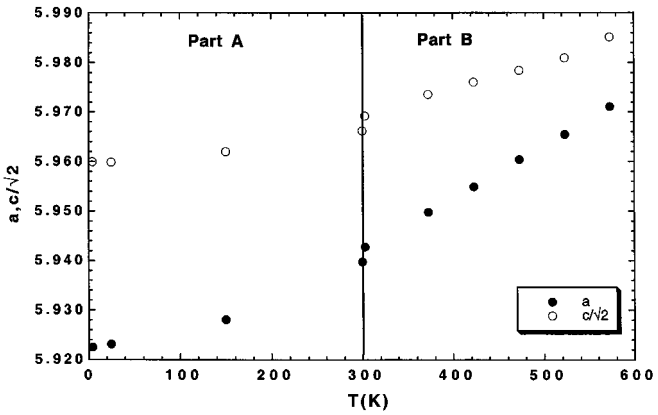

FIG. 5. Variation of a and $c/\sqrt{2}$ as a function of temperature for $Sr_{0.4}K_{0.6}BiO_3$. Parts A and B correspond to the low and high temperature experiments, respectively.

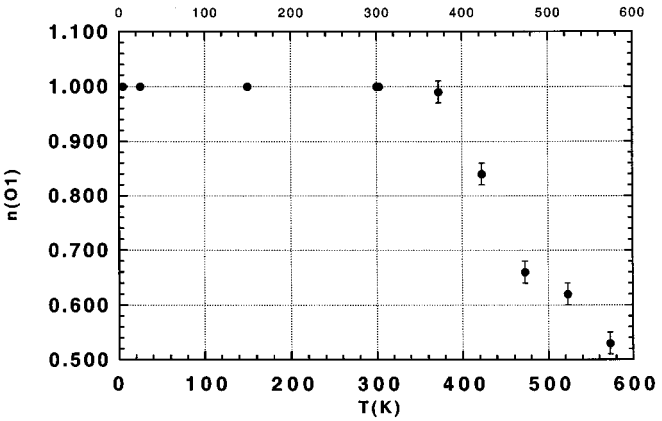

FIG. 6. Variation of the occupation factor of the O1 site in $Sr_{0.4}K_{0.6}BiO_3$ as a function of temperature.

This oxygen departure corresponds to a stoichiometry variation between $Sr_{0.4}K_{0.6}BiO_3$ and $Sr_{0.4}K_{0.6}BiO_{2.53}$. The Bi average valence changes correspondingly between $+4.6$ and $+3.7$. When the O1 site is fully occupied, the Bi cations are located in an almost regular octahedron. If one takes into account the standard deviations, the Bi–O distances remain constant up to 573 K (Table 5). As the oxygen stoichiometry decreases, a larger number of the Bi cations become pyramidally coordinated. At 573 K, the oxygen stoichiometry is such that all Bi cations would be five-coordinated. This situation corresponds to the limit of the phase stability in air. If the temperature is increased beyond this value, the phase begins to decompose, probably because an extra oxygen departure would result in a square-planar coordination for some of the Bi cations, which is not a common configuration.

CONCLUSION

The structure of $Sr_{1.25}Bi_{0.75}O_3$ and $Sr_{0.4}K_{0.6}BiO_3$ have been determined from low temperature to decomposition. In both cases, the distortion from cubic symmetry decreases when T increases, however, no structural transition occurs. This is a noticeable difference with the case of Ba-based bismuthates ($BaPb_{1-x}Bi_xO_3$ and $Ba_{1-x}K_xBiO_3$). We know that for $BaBiO_3$, the decomposition temperature is above 1300 K. Below that, two structural phase transitions occur: at 405 K from monoclinic to rhombohedral, and around 750 K to cubic. In the case of $Sr_{1.25}Bi_{0.75}O_3$, the decomposition temperature is much lower, indicating the lower stability of the phase, and it may occur before any structural transition. For doped samples, $Sr_{1-x}K_xBiO_3$ can be compared only to $BaPb_{1-x}Bi_xO_3$ since $Ba_{1-x}K_xBiO_3$ is already cubic at room temperature. $BaPb_{1-x}Bi_xO_3$ undergoes a structural phase transition at about 720 K from tetragonal to cubic. $Sr_{1-x}K_xBiO_3$ is already decomposed at this temperature, which again may explain the absence of any structural phase transition.

In the case of the superconducting K-doped sample, it has been possible to observe a regular decrease of the oxygen content, which had not been detected from TGA experiments under Ar atmosphere, probably because the heating rate was too fast. By changing the oxygen stoichiometry, we are able to modify the electronic doping of the sample in a different way than by varying the K content. These two approaches should be, however, quite different because the former has a strong effect on the Bi site probably by creating localization centers for Bi^{3+} on the pyramidally coordinated sites, whereas the latter has a more indirect influence. In the case of Ba-based bismuthates, the decrease of oxygen stoichiometry was reported to induce a decrease of T_c (12). We are now preparing samples, having defined

TABLE 5
Bi–O Interatomic Distances (Å) for $Sr_{0.4}K_{0.6}BiO_3$ from 4 to 573 K

T (K)	573	523	473	423	373	303	293	150	25	4
Bi–O1 × 2	2.11576(8)	2.11427(8)	2.11337(7)	2.11252(6)	2.11166(6)	2.11010(5)	2.10898(5)	2.10753(5)	2.10675(5)	2.10659(5)
Bi–O2 × 4	2.11(4)	2.11(3)	2.12(2)	2.11(3)	2.11(3)	2.11(2)	2.11(2)	2.110(2)	2.109(2)	2.111(2)
Average Bi–O	2.11	2.11	2.12	2.11	2.11	2.11	2.111	2.109	2.108	2.110

TABLE 6
Positional and Thermal Parameters for $Sr_{0.4}K_{0.6}BiO_3$ at High Temperatures (Space Group *I*4/*mcm*)

T (K)		303	373	423	473	523	573
a (Å)		5.94277(5)	5.94977(5)	5.95493(6)	5.96045(6)	5.96550(6)	5.97122(5)
c (Å)		8.4404(1)	8.4466(1)	8.4508(1)	8.4545(2)	8.4581(2)	8.4648(2)
Sr 4*b*	*x*	0	0	0	0	0	0
	y	0.5	0.5	0.5	0.5	0.5	0.5
	z	0.25	0.25	0.25	0.25	0.25	0.25
	B (Å^2)	1.08(5)	1.14(5)	1.30(5)	1.43(6)	1.49(6)	1.71(6)
Bi 4*c*	*x*	0	0	0	0	0	0
	y	0	0	0	0	0	0
	z	0	0	0	0	0	0
	B (Å^2)	0.25(2)	0.32(1)	0.37(2)	0.43(2)	0.44(2)	0.52(2)
O1 4*a*	*x*	0	0	0	0	0	0
	y	0	0	0	0	0	0
	z	0.25	0.25	0.25	0.25	0.25	0.25
	n	1.0	1.0	0.84	0.66	0.62	0.53
	B (Å^2)	2.7(8)	2.9(9)	2.3(4)	1.7(4)	2.0(4)	2.5(4)
O2 8*h*	*x*	0.224(3)	0.231(5)	0.228(4)	0.227(4)	0.235(6)	0.24(1)
	y	0.724(3)	0.731(5)	0.728(4)	0.727(4)	0.735(6)	0.74(1)
	z	0	0	0	0	0	0
	B (Å^2)	2.3(5)	3.0(6)	2.3(4)	1.7(4)	2.0(4)	2.5(4)
R_{wp} (%)		14.6	14.8	15.7	17.0	17.3	15.9
R_{Bragg} (%)		3.7	3.3	3.8	4.3	4.5	4.3

oxygen stoichiometries between O_3 and $O_{2.5}$, in order to follow the variation of T_c as well as the possible presence of superstructure reflexions or short-range ordering. We have already reported (13) the presence of diffuse scattering during the observation of samples by electron diffraction. This has been attributed to a small oxygen departure under the electron beam, by analogy to what was observed in Ba-based bismuthates (14).

ACKNOWLEDGMENTS

We thank J. L. Tholence and M. Nunez-Regueiro for a.c. susceptibility and resistivity measurements on the samples. This work was supported by RFBR-PICS (Grant 98-03-22007).

REFERENCES

1. L. R. Mattheiss, E. M. Gyorgy, and D. W. Johnson, *Phys. Rev. B* **37,** 3745 (1988).
2. S. M. Kazakov, C. Chaillout, P. Bordet, J. J. Capponi, M. Nunez-Regueiro, A. Rysak, J. L. Tholence, P. G. Radaelli, S. N. Putilin, and E. V. Antipov, *Nature* **390,** 148 (1997).
3. S. Pei, J. D. Jorgensen, B. Dabrowski, D. G. Hinks, D. R. Richards, A. W. Mitchell, J. M. Newsam, S. K. Sinha, D. Vaknin, and A. J. Jacobson, *Phys. Rev. B* **41,** 4126 (1990).
4. D. E. Cox and A. W. Sleight, *in* "Proc. Conf. Neutron Scattering" (R. M. Moon, Ed.), Gatlinburg, TN, June 6–10, 1976.
5. D. Mercurio, J. C. Champarnaud-Mesjard, B. Frit, P. Conflant, J. C. Boivin, and T. Vogt, *J. Solid State Chem.* **93,** 228 (1990).
6. S. Kazakov, Ph. D. thesis, Grenoble, France, 1998.
7. J. Rodriguez-Carvajal, *Physica B* **192,** 55 (1993).
8. Finger, Cox, and Jephcoat, *J. Appl. Crystallogr.* **27,** 892 (1994).
9. N. F. Brese and M. O'Keeffe, *Acta Crystallogr. Sect. B* **47,** 192 (1991).
10. T. N. Nguyen, D. M. Giaquinta, W. M. Davis, and H. -C. zur Loye, *Chem. Mater.* **5,** 1273 (1993).
11. C. Chaillout, G. J. Mc Intyre, J. Marcus, and M. Marezio, *Physica C* **185–189,** 2723 (1991).
12. M. Suzuki and T. Murakami, *Solid State Commun.* **53,** 691 (1985).
13. C. Chaillout, S. Kazakov, H. Schwer, E. M. Kopnin, P. Bordet, S. Pachot, E. V. Antipov, and J. J. Cappon, *in* "High Temperature Superconductors and Novel Inorganic Materials" (G. Van Tendeloo *et al.*, Eds.), pp. 103–108. Kluwer Academic, Dordrecht/Norwell, MA, 1999.
14. E. A. Hewat, C. Chaillout, M. Godinho, M. F. Gorius, and M. Marezio, *Physica C* **157**(2), 228 (1989).